# ISOTOPIC AND SOLAR GEOCHRONOLOGY AND CLIMATOSTRATIGRAPHY OF THE LATE PLEISTOCENE OF NORTHERN EURASIA

**© 2025 V. M. Fedorov***

*Lomonosov Moscow State University (MSU), Moscow, Russia*

**e-mail: fedorov.msu@mail.ru*

Received January 07, 2025

Revised January 19, 2025

Accepted April 14, 2025

**Abstract.** The possibility of explaining the causes of global climatic changes in the Late Pleistocene of Northern Eurasia on the basis of the astronomical theory of climate change is shown. In the Late Pleistocene, the effect of dividing seasonal radiation intensity by phases of annual Earth radiation intensity was found, which explains the mechanism of manifestation of the 100-millennial cycle in the Earth's natural system. Solar tuning (modeling) of the climatic epochs of the Late Pleistocene of Northern Eurasia has been performed. Based on the model, the solar conditions and the mechanism of development of cover glaciations in Northern Eurasia in the Late Pleistocene are determined. The cause of global climate change is related to the dynamics of the radiation factor, the representative characteristics of which are the intensity of summer radiation and the intensity of winter meridional radiation heat transfer in the Northern Hemisphere. The chronological discrepancies between the model and actual climatic epochs, reflecting the nonlinear response of the natural system to the dynamics of irradiation, average about 7 thousand years. There is a weak response of the oxygen isotope composition ($\delta^{18}O$) of bottom foraminifera (maximum range of 0.2% fluctuations) to fluctuations in radiation factors of global climatic changes in Northern Eurasia.: the intensity of summer radiation in the phase division of seasonal radiation (the average range for the summer half–year is 0.486%, for July - 0.785%) and in the phases of climatic precession (the average range is 4.336%).

**Keywords:** *astronomical theory of climate, solar climate, Late Pleistocene, Northern Eurasia, scheme of geochronology and climatostratigraphy, solar tuning/model*

**DOI:** 10.31857/S00167940250413e7

## 1. INTRODUCTION

The beginning of the history of the development of the astronomical theory of climate dates back to the middle of the XIX century and is associated with the works of J. Adhémar [Adhémar, 1842], which formulated the idea that the main cause of ancient glaciations could be violations in the regular course of the Earth's revolution around the Sun. The ideas about the connection of the periods of ancient glaciations with astronomical processes were also developed in the works of the Scottish scientist J. Croll [Croll, 1867; 1875]. The change in the eccentricity of the Earth's orbit is taken as a fundamental astronomical factor in Croll's ideas (along with the precession cycle). Later, the mathematical part of the problem, taking into account three astronomical parameters (eccentricity, ecliptic inclination, precession) affecting the Earth's irradiation, was investigated in the works of M. Milankovitch [Milankovitch, 1939].

The astronomical theory of climate change created about 100 years ago by M. Milankovitch in its existing form does not explain global climatic events that occurred in the Neopleistocene. Therefore, it needs modernization and development. Modernization includes performing irradiance calculations with high spatial and temporal resolution. The development of the astronomical theory of climate change includes a different approach to the transition from a solar climate to a global climate. To search for the causes of global climatic events in the Neopleistocene, we use periodicities in the dynamics of irradiation intensity of the entire Northern Hemisphere. Traditionally, our predecessors took into account periodicities in irradiance at the 65º N parallel, without arguing for its climatic representation for the Earth and hemispheres [Vernekar, 1972; Sharaf and Budnikova, 1969; Berger, 1978; Berger and Loutre, 1992; Laskar et al., 1993]. The fundamental differences are manifested by the fact that hemispheric irradiance is determined by three secular variations in incoming radiation. These are about 400-thousand-year variation in eccentricity, a 100-thousand-year periodicity associated with eccentricity modulation of seasonal irradiance, and about 22-thousand-year periodicity reflecting climatic precession (or the dynamics of perihelion longitude) [Fedorov, 2024]. In this case, the periodicity associated with the change of the axis tilt (41 thousand years on average), which regulates the irradiation intensity in certain 5-degree latitude zones, areas of source and sink of radiative heat, and at certain parallels (in particular, at 65º N), is not manifested. The paper assumes that the causes of global climatic changes in the Northern Hemisphere are related to the dynamics of irradiation of the entire hemisphere, rather than a separate 65º N parallel. Another element in the development of the astronomical theory of climate change is the calculation of solar characteristics that regulate the transfer of radiative heat at the upper boundary of the atmosphere. This is insolation contrast (IC), which generalizes over the source and sink regions of radiative heat and reflects the change in the meridional gradient of insolation, which in the natural system regulates the transfer of heat from

low latitudes to high latitudes ("heat machine of the first kind") [Shuleykin, 1953]. Insolation seasonality (IS) - which regulates heat transfer in the ocean-continent system associated with the seasonal change of heat source and sink areas ("heat machine of the second kind") [Monin, 1982]. Insolation seasonality of the Earth (ISE), which regulates the interhemispheric transfer of radiative heat from the summer hemisphere to the winter hemisphere. Thus, the astronomical theory is supplemented with previously not calculated and not taken into account characteristics of radiative heat transfer, variations of which are also factors of global climate change, as well as variations of incoming radiation (its intensity). The aim of the work is to improve the astronomical theory of climate change and search for the causes of global climatic changes in the Neopleistocene.

## 2. BASICS OF ASTRONOMICAL CLIMATE THEORY

To explain periodically recurring glaciation/interglaciation cycles in the Quaternary period and to physically substantiate the glacial theory, M. Milankovitch proposed an astronomical theory of climate fluctuations more than a century ago. He accepted summer insolation at 65º N as a solar criterion for climate change (but the climatic representativeness of 65º N irradiance was accepted without proof). The insolation was calculated for this parallel 650,000 years into the past and was generally consistent at that time with the scheme of glaciation/interglaciation cycles developed by A. Penck and E. Brickner for the Alps. However, later, with the appearance of new paleogeographic data and the development of absolute dating methods, the previously identified consistency in the dynamics of exposure and stratigraphy of glacial and interglacial deposits was broken. In its existing form, the astronomical climate theory does not explain global changes in the natural environment in the Neopleistocene

**Figure 1.**

Further development of the astronomical theory of climate change proceeded in two directions. One direction is associated with repeated calculations of irradiation due to the appearance of new astronomical data on the masses and motion parameters of bodies in the Solar System [Brouwer and Van Woerkom, 1950; Vernekar, 1972; Sharaf and Budnikova, 1969; Berger and Loutre, 1992; Laskar et al., 1993] (Fig. 1). At the same time, the summer irradiation of the Earth at 65º N was still considered representative for explanation of global climatic changes. The equivalent latitudes for 65° N are understood to be the latitudes at which the same amount of solar radiation is currently received during the summer caloric half-year as was received at latitude 65° N in the past. An increase in equivalent latitude means a decrease in incoming radiation and vice versa. Caloric half-years are defined as half-years of equal duration$\left(\frac{T_o}{2}\right)$, when at a given latitude

any value of daily insolation in the summer half-year is greater than any value of daily insolation in the winter half-year.

Another direction in the development of astronomical climate theory is associated with the emergence of tuning technology or orbital tuning. Insolation (solar) or orbital tuning refers to the process of matching sedimentary cycles with orbital periodicity, which determines long-period variations in insolation, to estimate the timing and duration of global key events in the Earth's geologic history [Malinverno et al., 2010]. Orbital adjustment is typically a mathematical technique for adjusting the time scale of the geologic or climate record to achieve maximum synchronization with the cycles of orbital motion (or irradiance) characteristics represented in astronomical climate theory [Imbrie and Imbrie, 1988; Bolshakov, 2003]. Oxygen isotope (OI) scales that currently form the basis of Pleistocene geochronology and climatostratigraphy [Hays et al., 1976; Imbrie et al., 1984; Bassinot et al, 1994; Lisiecki and Raymo, 2005] are tuned from summer insolation curves (the main external energy signal) calculated for 65º N or from astronomical characteristics (eccentricity, perihelion longitude, and tilt of the rotation axis) that regulate the Earth's irradiance. The IR scales thus represent the IR response ($\delta^{18}O$) tuned by a solar (or astronomical) factor, i.e., they are the result of orbital or solar tuning [Malinverno et al., 2010; Fedorov, 2021a]. The IR indicator ($\delta^{18}O$) is determined from the ratios of light and heavy oxygen isotopes.

The development of powerful continental glaciations, their disappearance, the lowering and raising of the global ocean level by 100 and more meters, and the formation of thick strata of perennially frozen rocks are reflected by changes in $\delta^{18}O$ in the LR04 scheme in a very narrow range of values [Lisiecki and Raymo, 2005] - from 2 ‰ (or 0.2%) in the Neopleistocene to 1 ‰ (or 0.1%) at earlier times. Nevertheless, the IR response ($\delta^{18}O$), isolated from the factor (solar radiation) of global changes occurring on the Earth's surface by 3-4- kilometers thick ocean, is currently the basis of Neopleistocene geochronology and climatostratigraphy (marine isotope stages - MIS)

Recall that the astronomical theory of climate, which is based on two fundamental physical interactions - gravitational and electromagnetic, in its existing form, does not explain the global changes in the natural environment in the Neopleistocene. The IR scales record an extremely weak response to global changes in the natural environment. Consequently, the search for new criteria of the Earth's solar climate change in the Neopleistocene, objectively reflecting and explaining global paleogeographic events: the origin and development of continental glaciations and interglaciations, becomes urgent

## 3. INSOLATION CALCULATION METHODOLOGY

Calculations of annual and seasonal insolation (irradiation intensity - IE) for the Earth and hemispheres were performed. The calculations were based on the model of J. Laskar [Laskar et al. Laskar [Laskar et al., 2004; 2011], which describes the smooth (without short-period oscillations) orbital motion and rotation of the Earth. Laskar's data (eccentricity of the Earth's orbit, angle of inclination of the Earth's axis, perihelion longitude) for the interval from -50 million to +20 million Julian years relative to the year 2000 with a step of 1000 years, available on the electronic resource (https://vo.imcce.fr/insola/earth/online/earth/La2004/index.html), were interpolated with a step of 500 years.

According to the interpolated data of J. Laskar and his estimates of the displacement of the vernal equinox point, the orbital motion and rotation of the Earth corresponding to Kepler's second law were reconstructed in tropical years, which are 800 thousand Julian years into the past from the year 2000 with a step of 500 years. In this case the duration of the sideric year was considered equal to 365.256363 SI days. For the nodal moments of tropical years (24 moments for each tropical day), the Sun's declination and the Sun-Earth distance were calculated.

The Earth's surface was approximated by an ellipsoid with an axis aligned with the Earth's rotation axis, with semi-major axis lengths of 6,378,137 m (major) and 6,356,752 m (minor), which corresponds to the parameters of the Geodetic Reference System 1980 (GRS80) Earth ellipsoid. All irradiation characteristics of the Earth surface and its parts were calculated based on the irradiation energies of latitudinal zones. The irradiation energy (J) of the latitudinal zone$(\varphi_1, \varphi_2)$ in the time interval$(t_1, t_2)$ was calculated by the formula:

$$\mathrm{EO}(\varphi_1, \varphi_2, t_1, t_2) = \int_{t_1}^{t_2} \int_{\varphi_1}^{\varphi_2} \sigma(\varphi) \int_{-\pi}^{\pi} \Lambda(t, \varphi, \alpha) d\alpha \, d\varphi \, dt \ , (1)$$

where α is the hour angle of the Sun (in radians) at time *t* (measured in SI seconds) at point P with geodetic latitude φ (in radians) located on the Earth's surface; σ(φ) is the area multiplier at point P; σ(φ)dαdφ is the area ($m^{2)}$ of an infinitesimal trapezoid centered at point P (the trapezoid is a surface cell);$\Lambda(t, \varphi, \alpha)$ is the irradiation intensity ($W/m^{2)}$ of this trapezoid in a small neighborhood of moment *t*. The calculation of σ(φ) and$\Lambda(t, \varphi, \alpha)$ was performed using the Sun's declination and the Sun-Earth distance in accordance with the previously developed methodology [Fedorov and Kostin, 2020]. The influence of the atmosphere and changes in the Sun's activity were not taken into account. The value of the solar constant (multiyear average TSI - Total solar irradiance) was assumed to be 1361 $W/m^2$ [Koop and Lean, 2011].

.

## 4. MAIN CRITERIA OF SOLAR CLIMATE CHANGE NEOPLEISTOCENE

It follows from earlier studies that the arena of occurrence and development of global climatic events in the Neopleistocene is the Northern Hemisphere [Fedorov and Frolov, 2024]. Since the climatic representativeness of the 65º N irradiation has not been determined, the irradiation characteristics of the entire Northern Hemisphere were taken as criteria. The intensity of annual and seasonal irradiation (SI) of the Earth and hemispheres was calculated. The annual irradiation intensity of the Earth and hemispheres are characterized by equal numerical values (since the area of the Earth is twice as large as the area of the hemisphere). The average value of the annual IE of the Earth and hemispheres in the Neopleistocene is 340.107 W/m$^2$. The maximum value is 340.391 W/m$^2$, the minimum is 339.959 W/m$^2$ (Fig. 2)

**Figure 2.**

Thus, the maximum magnitude of changes in the annual EI in the Neopleistocene is 0.432 W/m$^2$ (0.127%), which is commensurate with the maximum magnitude of the $\delta^{18}O$ indicator (about 0.2%) in the Neopleistocene. The annual EI of the Earth and hemispheres is closely related to changes in the eccentricity of the Earth's orbit (the correlation coefficient is 0.977). The climatic effect of eccentricity dynamics was first noted in the works of J. Croll [Croll, 1867; 1875].

The change in the intensity of seasonal exposure in the Neopleistocene was analyzed (Fig. 3).

**Figure 3.**

The average value of summer EI in the Northern Hemisphere is 426.414 W/m$^2$. The maximum value of the summer EI is 456.597 (220 thousand years ago) W/m$^{(2)}$, the minimum is 398.513 W/m$^2$ (231 thousand years ago). The maximum range of variation of summer IE is determined as 58.085 W/m$^2$ (13.622% of the long-term average of summer IE in the Neopleistocene). The correlation of the extremes of the summer IE in the Northern Hemisphere with the perihelion longitude is 0.894, and the amplitude (modulus of deviation from the mean) of the summer IE with the eccentricity is 0.954. That is, the extrema of the summer IO are determined by the dynamics of perihelion longitude, and their amplitude is determined by the dynamics of eccentricity (Fig. 4).

**Figure 4.**

**Table 1.**

We studied the distribution of seasonal IE by phases of increase and decrease of annual IE (the dynamics of which is determined by the eccentricity) (Table 1).

The average value of summer IE in the phases of the annual IE increase in the Northern Hemisphere is 427.391 W/m$^2$, in the phases of decrease - 425.318 W/m$^2$. Thus, the summer IE of the Northern Hemisphere in the phases of the increase of annual IE is on average by 2.073 W/m$^2$ greater than the summer IE of the Northern Hemisphere in the phases of the decrease of annual IE.

This is 0.486% of the mean value of the Northern Hemisphere summer IE for the Neopleistocene (426.414 W/m$^{2)}$. The average value of winter IE in the phases of the annual IE increase is 253.760 W/m$^2$, in the phases of decrease - 254.930 W/m$^2$. The intensity of winter irradiation of the Northern Hemisphere in the phases of the annual IE increase is 1.169 W/m$^2$ inferior to the winter IE in the phases of the annual IE decrease, which is 0.460% of the mean value of the winter IE for the Neopleistocene (254.280 W/m$^{2)}$.

In the Southern Hemisphere in the first astronomical half-year (winter in the Southern Hemisphere) in the phases of increase of annual IO the value of winter IO in average for a phase is 254.968 W/m$^2$, in the phases of decrease - 253.768 W/m$^2$. Consequently, in the phases of the increase of annual IO, the winter irradiation in the Southern Hemisphere exceeds the values of winter IO in the phases of the decrease of annual irradiation by an average of 1.2 W/m$^2$ (0.472%). In the second astronomical (summer in the Southern Hemisphere) semiannual period, the opposite situation is noted. In the phases of the increase of the annual MR, the summer MR averages 425.280 W/m$^2$, in the phases of the decrease of the annual MR - 427.252 W/m$^2$. That is, in the phases of the annual TO increase, the summer TO in the Southern Hemisphere is on average 1.973 W/m$^2$ (0.427%) less than in the phases of the annual TO decrease.

**Table 2.**

Thus, in the first astronomical half-year (summer in the Northern Hemisphere and winter in the Southern Hemisphere), there is a direct effect of separation of the seasonal irradiation of the hemispheres by the phases of the annual IO fluctuation. In the second astronomical half-year (winter in the Northern Hemisphere and summer in the Southern Hemisphere), the opposite effect is observed (Table 2).

On average, the phase separation is more than twice as large as the maximum magnitude of the $\delta^{18}O$ index (about 0.2%) in the Neopleistocene. If we consider the irradiation intensity in July and January (the 4th and 10th astronomical months), the magnitude of changes in the phases of increase or decrease of the annual IO (these phases are named by us as solarian epochs - SE) increases (Table 3).

**Table 3.**

On average, the phase separation of the July and January IO is almost 4 times the maximum extent of the $\delta^{18}O$ index in the IR scale - LR04 scheme [Lisiecki and Raymo, 2005] in the Neopleistocene.

The phase separation effect is related to the fact that the dynamics of eccentricity (which determines the fluctuations of the annual EI of the Earth and hemispheres with an average period of about 100 thousand years) modulates the change in the amplitude of seasonal EI in the hemispheres. When the eccentricity of the Earth's orbit increases, the amplitude of fluctuations of seasonal

(summer and winter) EI in the hemispheres increases. At decreasing eccentricity, the range of fluctuations of seasonal IO decreases. The effect of separation of seasonal exposure allows us to distinguish warm and cold epochs (with an average duration of about 50 thousand years) in the Earth's solar climate and explain the mechanism of the 100-thousand-year cycle in the dynamics of natural environment components. In the hemispheres, warm and cold (accepted by summer irradiation) solar epochs manifest themselves asynchronously. Based on the effect of seasonal separation in the solarian climate of the Earth in the Neopleistocene (based on the summer IO of the Northern Hemisphere as a criterion), 7 warm and 9 cold solarian epochs are distinguished, which can form the basis of solarian geochronology and climatostratigraphy of the Neopleistocene

Warm and cold epochs of the solar climate are superimposed on the summer IO fluctuation associated with climatic precession (with a period of about 22 thousand years on average). Climatic precession reflects the process of variation of summer IO in the Northern Hemisphere, associated with extreme differences in summer irradiation at the position of the Earth near the perihelion and aphelion of the orbit during the summer solstice. The first case corresponds to the maximum of summer irradiation, the second - to the minimum (these extremes are repeated on average in 11 thousand years) (Fig. 3). The climatic effect of precession was first studied by J. Adhémar [Adhémar, 1842].

The values of the summer IO anomaly in the phases of climatic precession (CPP) in the Neopleistocene are limited to the range from 18.626 W/m$^2$ (4.358% of the long-term average for the Neopleistocene) to− 18.438 W/m$^2$ (− 4.324%). The maximum range of variation in the summer MR anomaly is 37.064 W/m$^2$ (8.692%). The mean positive deviation from the mean multiyear is 9.337 W/m$^2$ (2.190% of mean summer MR for the Neopleistocene - 426.414 W/m$^{(2)}$), and the negative deviation is 9.153 W/m$^2$ (2.147%). Consequently, the average difference in irradiance between the warm and cold phases of climatic precession averages 18.490 W/m$^2$ (4.336%), and the maximum is almost twice as large. Thus, the average magnitude of variations of the summer EI anomaly in the Northern Hemisphere is 21.7 times larger than the maximum magnitude of $\delta^{18}O$ indicator tuned by the 65º N irradiance in the Neopleistocene (about 0.2%).

In general, the variations of the seasonal irradiance of the Northern (and Southern) Hemisphere are related to the dynamics of the perihelion longitude, which is determined by the climatic precession (with a period of about 22 thousand years). The amplitude of fluctuations of seasonal IE in the cycles of climatic precession is modulated by the dynamics of eccentricity (with an average period of about 100 thousand years). The variations in the intensity of solar radiation arriving to the hemispheres are determined by the combination of these two oscillations. The tilt of the rotation axis (which varies with an average period of about 41 thousand years) changes the distribution of this radiation over latitudinal zones. When the tilt of the axis decreases, low latitudes

receive more solar energy, and when the tilt increases, high latitudes receive more. In the dynamics of the solar climate of the Earth and hemispheres this fluctuation is not manifested (it is manifested only in the dynamics of irradiation of separate latitudinal parallels and zones, for example, in irradiation at 65º N).

## 5. SETTING UP A SCHEME OF GEOCHRONOLOGY AND CLIMATOSTRATIGRAPHY NEOPLEISTOCENE OF NORTHERN EURASIA

On the basis of the noted periodicities in the change of solar climate, the climatostratigraphic scheme of the Neopleistocene of Northern Eurasia [Bolikhovskaya, 2007] was adjusted (solar adjustment or modeling) based on spore-dust analysis data obtained as a result of long-term studies of Pleistocene sediments and the results of absolute dating of skeletal remains of malacofauna (EPR method). For warm (interglacials) and cold (glaciations) climatic stages of the geochronological scheme [Bolikhovskaya, 2007], the mean values of summer IE in the Northern Hemisphere and the mean values of the summer IE anomaly were calculated for climatic epochs. In the scheme under consideration, 21.429% of climatic epochs agree by sign with the radiation factor (the solar criterion - the anomaly of the summer IO in the Northern Hemisphere), and 78.571% do not agree (Table 4). That is, in warm climatic epochs negative and in cold climatic epochs positive values of the mean for the climatic epoch anomaly of the summer IE are noted. For consistency of the energy impact factor and the response to it, the scheme was adjusted.

**Table 4.**

The customization was based on adopting the following rules as criteria:

- cold climatic epoch should generally begin and end with cold phases of climatic precession (CPP);
- warm climate epochs should generally begin and end with warm FCPs.

These criteria follow from the assumptions adopted for the model about the direct connection between temperature changes and changes in incoming solar radiation (although in reality this is not the case). In this work, we proceed from the assumption that the paleogeographic data are reliable, and the inconsistency noted (Table 4) is determined by the nonlinear response of the natural system to irradiation dynamics and possible errors in stratigraphic dissection, stratigraphic correlation of sediments, and determination of their absolute age.

The adjustment procedure was reduced to the fact that the boundaries of warm (cold) climatic epochs were shifted to the beginning and end of the nearest warm (cold) PCE at the beginning and end of the warm (cold) climatic epoch. As a result of the adjustment, the boundaries of climatic epochs shifted into the past or into the future by about 7 thousand years on average. This amounts to about 13% of the average duration of a climatic epoch. In [Bolikhovskaya, 2007], the

errors of the EPR method of absolute dating are not given. There is also no data on the magnitude of inevitable chronological errors both during stratigraphic dissection and correlation of sediments in individual geological sections and due to the generalization of data on sections in the compilation of a consolidated scheme of geochronology and climatostratigraphy of Northern Eurasia. The offsets can be associated not only with the noted possible errors, but also determined by the nonlinear response of the natural system to the energy signal entering it. Taking this into account, the obtained estimates of the tuning (modeling) bias can be considered satisfactory. These values reflect possible in nature shifts of climatic epochs relative to the periods of positive or negative anomalies of summer irradiation of the Northern Hemisphere.

As a result of the correction performed according to the adopted criteria, a model with a full correspondence of warm climatic epochs to the periods with positive mean anomalies of summer IE and cold climatic epochs to the periods with negative anomalies was obtained (Table 4). Obtained on the basis of the direct dependence of climatic epochs on the
of the Northern Hemisphere summer IO dynamics, the idealized model allows us to determine the solar conditions and the reasons for the change of climatic epochs in the Neopleistocene.

## 6. SOLARIAN CONDITIONS AND CAUSES OF ORIGIN AND DEVELOPMENT COVER GLACIATIONS IN THE NEOPLEISTOCENE

For the climatic epochs (interglacials and glaciations) obtained as a result of the solar model construction, the average anomalies of characteristics of radiative heat transfer were calculated (Table 5).

**Table 5.**

Summer and winter insolation contrast (IC) was calculated for the Northern Hemisphere as characteristics of the meridional transport intensity ("heat machine of the first kind"). Summer IR is calculated as the difference of summer IR in the source region (0-55º N) and sink region (55-90º N) of radiative heat. Winter IR is calculated as the difference of winter IR in the source region (0-35º N) and sink region (35-90º N) of radiative heat. The IR generalized by heat source and sink regions reflects the change in the meridional insolation gradient, which regulates the meridional transport of heat and moisture in the Earth's natural system [Fedorov, 2021b; 2023].

The intensity of heat exchange in the ocean-continent system ("heat machine of the second kind") is governed by insolation seasonality [Shuleykin, 1953; Monin, 1982; Fedorov, 2023], which reflects seasonal contrasts of the solar climate in the hemispheres. The IS is calculated as the difference between the intensity of summer and winter irradiation of the hemisphere. The change in the IS in the Northern Hemisphere in the Neopleistocene is similar to the change in the summer IS (the correlation coefficient between them equal to 0.999).

The interhemispheric transfer of radiative heat is characterized by the insolation seasonality of the Earth (ISE). This characteristic regulates the transfer of radiative heat from the summer hemisphere to the winter hemisphere, which leads to smoothing of seasonal differences of solar energy (heat) in the hemispheres. ISH is determined from the relation ISH = (IO summer in the Southern Hemisphere - IO winter in the Northern Hemisphere) - (IO summer in the Northern Hemisphere - IO winter in the Southern Hemisphere) [Fedorov, 2023]. In this case, the positive values of ISH mean the dominance of radiative heat transfer from the summer Southern Hemisphere to the winter Northern Hemisphere over the transfer from the summer Northern Hemisphere to the winter Southern Hemisphere.

As a result, for the tuned (model) climatic epochs, a picture of close correlation relations of solar characteristics (their mean anomalies) was obtained. Thus, the average for model climatic epochs anomaly of summer IS has a close negative relationship with the average anomaly of winter IR (− 0.906) and ISP (− 0.965) and a close positive relationship with the average anomaly of IS (0.996). The winter IR, ISW and IS are also closely related to each other.

The ratios of solar characteristics obtained for the model climatic epochs determine the conditions under which glaciations and interglacials occur and develop. As follows from Table 5, the cold climatic epochs - glaciations (with negative anomalies of summer IS and IS) in the Northern Hemisphere correspond to the increased meridional transport of radiation heat in the winter half-year (positive mean anomalies of winter IS and ISW). Warm climatic epochs - interglacials (with positive mean anomalies of summer IR and IS) in the Northern Hemisphere correspond to the weakening of the meridional transfer of radiative heat in the winter half-year (negative mean anomalies of winter IR and IS). Note that the winter radiative heat transport in the Neopleistocene averages (211.868 $W/m^{2)}$ 3.063 times higher than the summer transport (69.174 $W/m^{2)}$ in the Northern Hemisphere. The obtained ratio of characteristics also allow us to determine the physical mechanism of glaciations and interglaciations.

The glacial epochs are characterized by negative values of the mean anomaly of the summer IR (and IS), to which low near-surface air and ocean surface temperatures should correspond. Also the glacial epochs are characterized by the positive values of mean anomaly of the winter IR (and IS). At the background of low summer irradiation, there is an increase in the meridional heat and moisture transport in the winter (for the Northern Hemisphere) half-year from low latitudes to high latitudes. The increase of atmospheric precipitation in the solid phase in the area of heat runoff can be connected with this process. Snow accumulation occurs, which due to low values of the summer IE does not have time to melt completely, firnization and subsequent transformation of firn into ice. The interglacial is characterized (Table 5) by the positive values of the average anomaly of the summer IE (and IS). Positive values of the mean IS anomaly characterize a more continental

climate, while negative values characterize a more maritime climate [Monin and Shishkov, 1979]. Since the mean anomaly of the summer IE is closely related to the mean IS anomaly (0.996), a warm climate (interglaciation) will be more continental, and a cold climate (glaciation) will be more maritime. Positive values of the summer IC anomaly may be an indicator of increased warming in the area of heat flow in the summer half of the year. Since the mean anomaly of the winter IR is closely related to the mean ISW anomaly (0.997), the winter meridional heat and moisture transport in the Northern Hemisphere is also enhanced by the transport of radiative heat and moisture from the summer Southern Hemisphere to the winter Northern Hemisphere.

Positive feedbacks that strengthen the cooling or warming trend should also be noted. They are primarily related to changes in albedo due to the increase (decrease) in the area of sea ice, cover and mountain glaciers, as well as duration of snow cover occurrence. Also important are the initial states of the natural system at the time of the onset of solar conditions contributing to the development of glaciations and interglaciations. This can determine the peculiarities in the development of these climatic events, the extent of their geographical distribution and shifts in time relative to the extremes of the solar climate characteristics.

It follows from all of the above that the change of glacial epochs in the Neopleistocene is caused by the dynamics of the solar climate, which is determined by the addition of fluctuations in the summer irradiation intensity of the Northern Hemisphere (determined by the dynamics of eccentricity and perihelion longitude) and the intensity of the winter radiative heat transfer (also mainly related to the dynamics of perihelion longitude). The noted discrepancies between model and actual climatic epochs, averaging about 7 thousand years, reflect the nonlinear nature of the relationship between changes in the state of the Earth's natural system and the dynamics of its irradiation and radiative heat transfer.

## 7. CONCLUSION

As a result of calculations of the Earth's irradiation intensity, a toolkit for solar tuning (modeling) of global and regional climatostratigraphic schemes of the Neopleistocene was obtained.

Adjustment (modeling) of the scheme of geochronology and climatostratigraphy of Northern Eurasia on the basis of solar characteristics reflecting variations in the input and transfer of radiation heat has been performed. Based on the energetic correspondence of warm and cold climatic epochs in the Neopleistocene in Northern Eurasia to the periods of positive and negative values of the mean anomaly of summer radiation intensity, respectively, a solar model of climatic epochs for the Neopleistocene was obtained. The mean anomaly of the Northern Hemisphere summer irradiance intensity integrally reflects irradiance variations related to the dynamics of

eccentricity and perihelion longitude. Estimates of chronological discrepancies between model and actual climatic epochs for the Neopleistocene are obtained.

The model is used to determine the solar conditions and the mechanism of development of cover glaciations in Northern Eurasia in the Neopleistocene. The causes of global climatic changes are related to the radiation factor, representative characteristics of which are the intensity of summer irradiation of the Northern Hemisphere and the winter meridional transfer of radiation heat in the Northern Hemisphere (synchronously with the ISE).

There is an extremely limited response of $\delta^{18}O$ changes, which does not adequately reflect the range of fluctuations in the intensity of summer irradiation of the Northern Hemisphere - a factor of global climatic changes. In this connection, the possibility of using the $\delta^{18}O$ indicator of the oxygen isotope composition of benthic foraminifera for geochronology and climatostratigraphy of the Neopleistocene (marine isotope stages - MIS) does not seem reasonable.

FUNDING

The work was prepared within the framework of realization of the state budgetary theme "Paleogeographic reconstructions of natural geosystems and forecasting of their changes" (121051100135-0).

REFERENCES

1. *Bolikhovskaya N.S.* Spatial and temporal patterns of vegetation and climate development in Northern Eurasia in the Neopleistocene // Archaeology, Ethnography and Anthropology of Eurasia. № 4 (32). C. 2-28. 2007.

2. *Bolshakov V.A.* New concept of the orbital theory of climate. Moscow: Moscow University, 256 p. 2003.

3. *Imbrie D., Imbrie K.P.* Secrets of Glacial Epochs. Moscow: Progress, 264 p. 1988.

4. *Melnikov V.P., Smulsky I.I.* Astronomical theory of ice ages: New approximations. Solved and unsolved problems. Novosibirsk: GEO, 98 p. 2009.

5. *Milankovich M.* Mathematical climatology and astronomical theory of climate fluctuations. M.-L.: GONTI, 208 p. 1939.

6. *Monin A.S.* Introduction to the theory of climate. L.: Gidrometeoizdat, 246 p. 1982.

7. *Monin A.S., Shishkov Y.A.* History of Climate. L.: Gidrometeoizdat, 408 p. 1979.

8. *Fedorov V.M.* Holocene paradox in the astronomical theory of climate and problems of orbital tuning // Geophysical processes and biosphere. T. 20. № 1. C. 95-104. 2021a. https://doi.org/10.21455/GPB2021.1-9

9. *Fedorov V.M.* Astronomical theory of climate: modernization and development issues // Hydrometeorology and Ecology. № 64. С. 435-465. 2021б. https://doi.org/10.33933/2713-3001-2021-64-435-465
10. *Fedorov V.M.* Problems of parameterization of the radiation block of physical and mathematical climate models and possibilities of their solution // Uspekhi physicheskikh nauki. Т. 193. № 9. С. 971-988. 2023. https://doi.org/10.3367/UFNr.2023.03.039339
11. *Fedorov V.M.* Isotopic and solar geochronology and climatostratigraphy of the Neopleistocene and Holocene / Proceedings of the XXVIII All-Russian Annual Conference on Solar Physics "Solar and Solar-Terrestrial Physics - 2014". Ed. A.V. Stepanov, Y.A. Nagovitsyn. SPb.: GAO RAS. С. 319-322. 2024. https://doi.org/10.31725/0552-5829-2024-319-322
12. *Fedorov V.M., Frolov D.M.* Solar geochronology of the Late Pleistocene and Holocene // Earth Cryosphere. 2024. Т. 28. № 2. С. 47-57. https://doi.org/10.15372/KZ20240205
13. *Sharaf Sh.G., Budnikova N.A.* Century changes in the Earth's orbit and astronomical theory of climate fluctuations // Proceedings of the Institute of Theoretical Astronomy, USSR Academy of Sciences. Vyp. 14. С. 48-84. 1969.
14. *Shuleykin V.V.* Physics of the Sea. Moscow: Academy of Sciences of the USSR, 990 p. 1953.
15. *Adhémar J.A.* Revolutions de la mer: déluges périodiques. Paris: Carilian-Goeury et V. Dalmont, 184 p. 1842.
16. *Bassinot F.C., Labeyrie L.D., Vincent E., Quidelleur X., Shackleton N.J., Lancelot Y.* The astronomical theory of climate and the age of the Brunhes-Matuyama magnetic reversal // Earth Planet. Sc. Lett. V. 126. N 1-3. P. 91-108. 1994. https://doi.org/10.1016/0012-821X(94)90244-5
17. *Berger A.* Long-term variations of daily insolation and Quaternary climatic changes // J. Atmos. Atmos. Sci. V. 35. N 12. P. 2362-2367. 1978. https://doi.org/10.1175/1520-0469(1978)035<2362:LTVODI>2.0.CO;2
18. *Berger A., Loutre M.F.* Astronomical solutions for paleoclimate studies over the last 3 million years // Earth Planet. Sc. Lett. V. 111. N 2-4. P. 369-382. 1992. https://doi.org/10.1016/0012-821X(92)90190-7
19. *Brouwer D., Van Woerkom A.J.J.* The secular variation of the orbital elements of the principal planets // Astronomical Papers. V. 13. P. 81-107. 1950.
20. *Croll J.* On the eccentricity of the Earth's orbit, and its physical relations to the glacial epochs // Philos. Mag. V. 33. N 221. P. 119-131. 1867. https://doi.org/10.1080/14786446708639757
21. *Croll J.* Climate and time in their geological relations: a theory of secular changes of the Earth`s climate. London: Edward Stanford, 577 p. 1875.

22. *Fedorov V.M., Kostin A.A.* The calculation of the Earth`s insolation for the 3000 BC - AD 2999 / Processes in GeoMedia. V. 1. Ed. T.O. Chaplina. Cham, Switzerland: Springer. P. 181-192. 2020. https://doi.org/10.1007/978-3-030-38177-6_20
23. *Hays J.D., Imbrie J., Shackleton N.* Variation in the Earth's orbit: pacemaker of the ice ages // Science. V. 194. N 4270. P. 1121-1132. 1976. https://doi.org/10.1126/science.194.4270.1121
24. *Imbrie J., Hays J.D., Martinson D.G., Mclntyre A., Mix A.C., Morley J.J., Pisias N.G., Prell W.L., Shackleton N.J.* The orbital theory of Pleistocene climate: Support from a revised chronology, of the marine$\delta^{18}O$ record / Milankovitch and Climate. Part 1. Eds. A. Berger, J. Imbrie, J. Hays, G. Kukla, B. Saltzman. Dordrecht: Springer. P. 269-305. 1984.
25. *Kopp G., Lean J.* A new, lower value of total solar irradiance: Evidence and climate significance // Geophys. Res. Lett. V. 37. N 1. ID L01706. 2011. https://doi.org/10.1029/2010GL045777
26. *Laskar J., Joutel F., Boudin F.* Orbital, precessional and insolation quantities for the Earth from - 20 Myr to + 10 Myr // Astron. Astrophys. V. 287. N 1-2. P. 522-533. 1993.
27. *Laskar J., Robutel P., Joutel F., Gastineau M., Correia A. C. M., Levrard B. A long-term numerical solution for the insolation quantities of the Earth // Astron. M., Levrard B.* A long-term numerical solution for the insolation quantities of the Earth // Astron. Astrophys. V. 428 N 1. P. 261-285. 2004. https://doi.org/10.1051/0004-6361:20041335
28. *Laskar J., Fienga A., Gastineau M., Manche H.* La2010: a new orbital solution for the long-term motion of the Earth // Astron. Astrophys. V. 532. ID A89. 2011. https://doi.org/10.1051/0004-6361/201116836
29. *Lisiecki L.E., Raymo M.E.* A Pliocene-Pleistocene stack of 57 globally distributed benthic$\delta^{18}O$ records // Paleoceanography. V. 20. N 1. ID PA1003. 2005. https://doi.org/10.1029/2004PA001071
30. *Malinverno A., Erba E., Herbert T.D.* Orbital tuning as an inverse problem: Chronology of the early Aptian oceanic anoxic event 1a (Selli Level) in the Cismon APTICORE // Paleoceanography and Paleoclimatology. V. 25. N 2. ID PA2203. 2010. https://doi.org/10.1029/2009PA001769
31. *Molodkov A., Bolikhovskaya N.* Eustatic sea-level and climate changes over the last 600 ka as derived from mollusc-based ESR-chronostratigraphy and pollen evidence in Northern Eurasia // Sedimentary Geology. V. 150. N 1-2. P. 185-201. 2002. https://doi.org/10.1016/S0037-0738(01)00275-5
32. *Vernekar A.* Long-period global variations of incoming solar radiation / Long-Period Global Variations of Incoming Solar Radiation / Meteorological Monographs. V. 12. Boston, MA: American Meteorological Society. P. 1-128. 1972. https://doi.org/10.1007/978-1-935704-34-8_1

Figure captions

Figure 1. Variation of insolation for the summer caloric half-year for latitude $65^{(o)\ of}$ the Northern Hemisphere according to the data of different researchers [Melnikov and Smulsky, 2009]:
(*a*) - [Milankovich, 1939]; (*b*) - [Brouwer and Van Woerkom, 1950]; (*c*) - [Sharaf and Budnikova, 1969]; *d* - [Berger and Loutre, 1992]. The time in million years from 1950 is plotted on the abscissa axis;
along the ordinate axis: (*a*, *b*, *c*) - insolation at equivalent latitudes during the summer half-year, (*d*) - mean monthly insolation in July W ($W/m^{2)}$.

Figure 2. Intensity of annual irradiation of the Earth (and hemispheres) in the Neopleistocene.

Figure 3. Variation of the Northern Hemisphere summer irradiation intensity in the Neopleistocene.

Figure 4. Modulus of deviation of summer irradiance (amplitude) at extremes in the Northern Hemisphere from the long-term mean for the Neopleistocene.

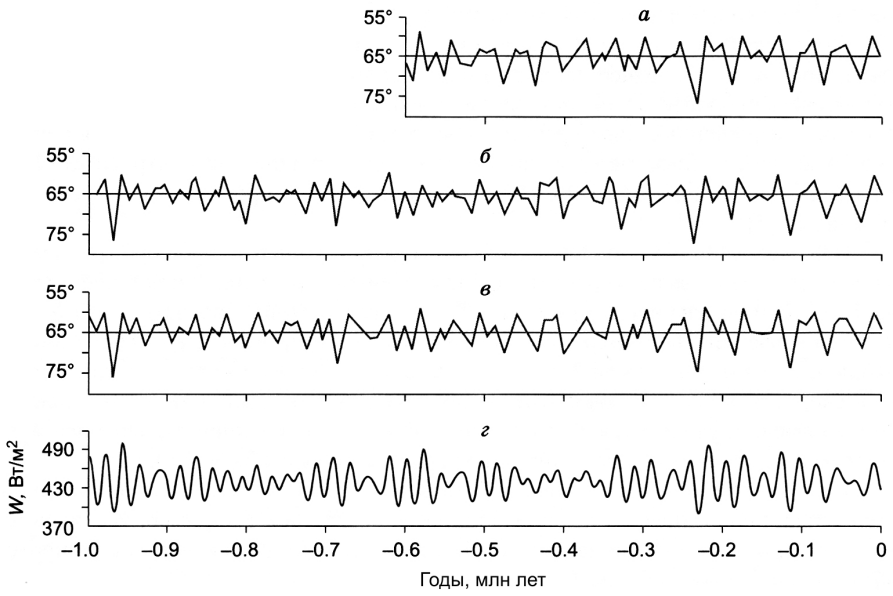


Figure 1.

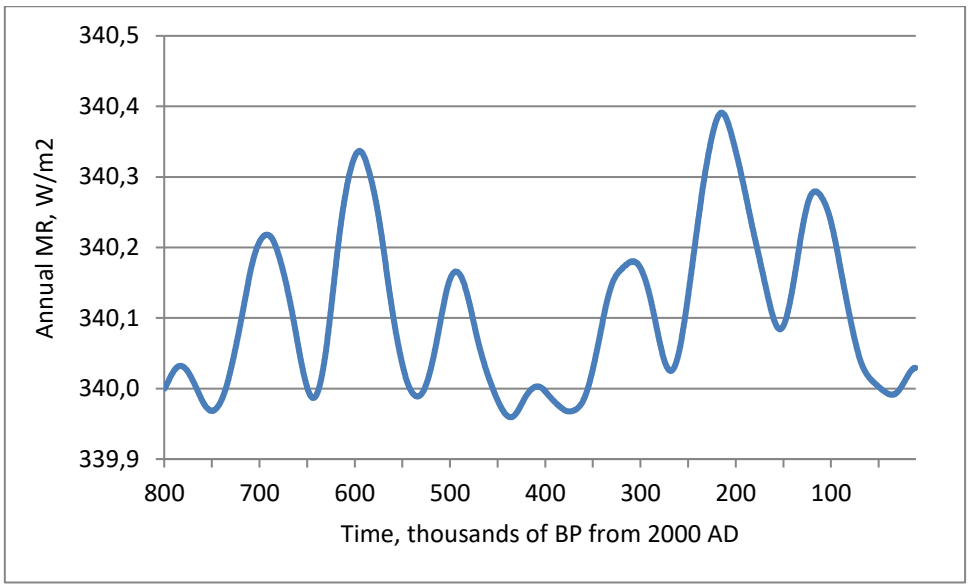


Figure 2.

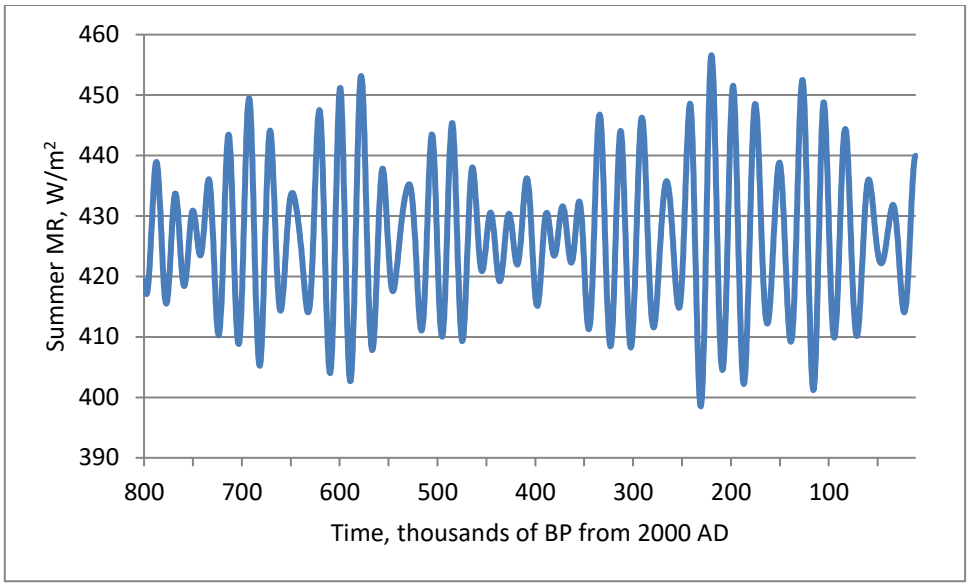


Figure 3.

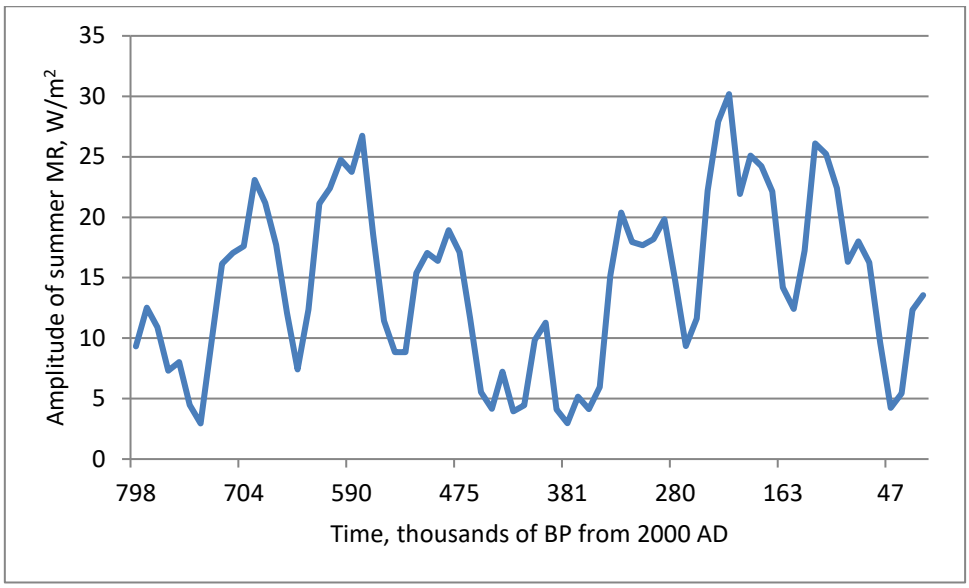


Figure 4.

Table 1. Mean values of seasonal irradiation of hemispheres in the phases of decrease and increase of annual irradiation intensity

| Phase of annual EI | Timing, thousands of years ago | Summer EI in JV, W/m$^2$ | Winter EI in JV, W/m$^2$ | Winter MR in SP, W/m$^2$ | Summer MR in SP, W/m$^2$ |
|---|---|---|---|---|---|
| Reductions | 782.0-750.0 | 424.296 | 255.358 | 254.062 | 426.530 |
| Increases | 749.5-693.0 | 427.344 | 253.523 | 254.124 | 426.309 |
| Reductions | 692.5-644.0 | 426.277 | 254.550 | 254.407 | 426.308 |
| Increases | 643.5-595.0 | 427.668 | 253.950 | 255.617 | 424.855 |
| Reductions | 594.5-534.0 | 425.062 | 255.149 | 252.991 | 428.653 |
| Increases | 533.5-495.0 | 426.448 | 254.274 | 254.530 | 425.873 |
| Reductions | 494.5-436.0 | 426.352 | 254.014 | 254.183 | 426.200 |
| Increases | 435.5-408.0 | 426.965 | 253.065 | 253.475 | 426.483 |
| Reductions | 407.5-374.5 | 425.128 | 254.975 | 254.686 | 425.425 |
| Increases | 374.0-308.0 | 427.357 | 253.648 | 254.917 | 425.203 |
| Reductions | 307.5-268.0 | 424.396 | 255.551 | 253.205 | 428.250 |
| Increases | 267.5-215.0 | 429.013 | 253.209 | 255.753 | 424.594 |
| Reductions | 214.5-153.5 | 425.021 | 255.462 | 252.761 | 429.547 |
| Increases | 153.0-117.0 | 428.363 | 253.456 | 255.363 | 425.065 |
| Reductions | 116.5-36.5 | 426.011 | 254.379 | 253.847 | 427.106 |
| Increases | 36.0-11.0 | 425.972 | 254.957 | 255.963 | 423.856 |

*Note.* Northern Hemisphere - Northern Hemisphere, Southern Hemisphere - Southern Hemisphere, the phases of increase of annual irradiation intensity are highlighted by the filler.

Table 2. Mean values of seasonal irradiation intensity separation in the hemispheres in the phase of the annual IE increase

| Northern Hemisphere | |
|---|---|
| Summer semester<br>+2.073 W/m$^2$ (0.486%) | Winter semester<br>-1.169 W/m$^2$ (− 0.460%) |
| Southern Hemisphere | |
| Winter semester<br>+1.2 W/m$^2$ (0.472%) | Summer semester<br>−1.973 W/m$^2$ (− 0.427%) |

Table 3: Average values of hemispheric irradiation separation in July and in January in the phase of increase of annual intensity

| Northern Hemisphere | |
|---|---|
| July<br>+3.687 W/m$^2$ (0.785%) | January<br>−1.593 W/m$^2$ (− 0.752%) |
| Southern Hemisphere | |
| July<br>+1.614 W/m$^2$ (0.763%) | January<br>−3.527 W/m$^2$ (− 0.750%) |

Table 4: Climatic epochs and their corresponding mean values of summer irradiation intensity and its anomalies

| Climatic epochs (interglaciation / glaciation) | Age range, Thousands of l.n.s. (by EPR) | Average summer MR, W/m$^2$ | Average anomaly of summer MR, W/m$^2$ | Age range, thousand hp (model) | Medium summer MR, W/m$^2$ | Average anomaly of summer MR, W/m$^2$ |
|---|---|---|---|---|---|---|
| | 759-787** | 425.603 | −0.811 | 764.0-793.0 | 428.160 | 1.746 |
| | 712-759 ** | 426.918 | 0.503 | 698.5-763.5 | 424.872 | −1.542 |
| Semilukskoe | 659-712** | 425.808 | −0.606 | 666.0-698.0 | 430.322 | 3.908 |
| Donskoe | 610-659* | 426.494 | 0.079 | 605.0-665.5 | 424.340 | −2.074 |
| Muchkapskoe | 535-610* | 426.422 | 0.008 | 523.5-604.5 | 428.215 | 1.795 |
| Oka | 455-535* | 426.803 | 0.389 | 469.5-523.0 | 424.449 | −1.990 |
| | 360-455* | 425.918 | −0.496 | 360.0-469.0 | 426.542 | 0.127 |

| | | | | | | |
|---|---|---|---|---|---|---|
| Kaluga | 340-360* | 422.570 | −3.844 | 340.5-359.5 | 422.432 | −3.982 |
| | 280-340* | 428.127 | 1.713 | 285.5-340.0 | 429.210 | 2.796 |
| Zhizdrinskoye | 235-280* | 427.709 | 1.295 | 248.5-285.0 | 422.848 | −3.566 |
| | 200-235 * | 424.197 | −2.217 | 193.0-248.0 | 429.786 | 3.372 |
| Dnieper | 145/140-200* | 428.006<br>426.962 | 1.592<br>0.548 | 133.5-192.5 | 423.600 | −2.815 |
| | 70-145/140* | 425.845<br>426.254 | −0.569<br>−0.160 | 78.0-133.0 | 427.930 | 3.223 |
| Valdai | 10-70* | 426.431 | 0.017 | 11.0-77.5 | 424.960 | −1.454 |

*Note.**From [Molodkov and Bolikhovskaya, 2002].**From [Bassinot et al., 1994].
Interglacial epochs are highlighted by the filler

Table 5. Solar characteristics of tuned (model) climatic epochs Northern Eurasia in the Neopleistocene

| Climatic epochs | Age range, Thousands of l.n.s. | Average anomaly, W/m$^2$ | | | |
|---|---|---|---|---|---|
| | | Summer EI | Winter IR | IP | ISR |
| Gremyachie Interglacial | 764.0-793.0 | 1.746 | −1.055 | 3.179 | −1.542 |
| Maiden Glaciation | 698.5-763.5 | −1.542 | 0.678 | −2.202 | 1.212 |
| Semiluk interglacial | 666.0-698.0 | 3.908 | −1.936 | 5.753 | −3.315 |
| Don glaciation | 605.0-665.5 | −2.074 | 1.188 | −3.159 | 1.838 |
| Muchkap interglacial | 523.5-604.5 | 1.795 | −0.650 | 2.746 | −1.198 |
| Ox glaciation | 469.5-523.0 | −1.990 | 0.652 | −3.414 | 1.176 |
| Likhvin interglacial | 360.0-469.0 | 0.127 | −0.259 | 0.807 | −0.178 |
| Kaluga cooling | 340.5-359.5 | −3.982 | 0.222 | −6.951 | 1.272 |
| Chekalinsky interglacial | 285.5-340.0 | 2.796 | −0.798 | 4.533 | −1.637 |
| Gisdrin cooling | 248.5-285.0 | −3.566 | 1.622 | −5.470 | 2.856 |
| Cherepetsk interglacial | 193.0-248.0 | 3.372 | −1.076 | 4.499 | −2.249 |
| Dnieper glaciation | 133.5-192.5 | −2.815 | 1.380 | −4.794 | 2.198 |
| Mikulin interglacial | 78.0-133.0 | 3.223 | −0.907 | 4.886 | −1.949 |
| Valdai glaciation | 11.0-77.5 | −1.454 | 0.101 | −2.142 | 0.556 |

*Note:* interglacials are marked by fillings.